Original Article
An immune-competent rat split thickness skin graft model: useful tools to develop new therapies to improve skin graft survival

Qiyi Zhai[1*], Fei Zhou[1*], Mohamed M Ibrahim[2], Jingling Zhao[1], Xusheng Liu[1], Jun Wu[1], Lei Chen[1], Shaohai Qi[1]

[1]Department of Burns Surgery, First Affiliated Hospital of Sun Yat-sen University, Guangzhou, Guangdong, China; [2]Division of Plastic and Reconstructive Surgery, Department of Surgery, Duke University Medical Center, Durham, NC, USA. *Equal contributors.

Abstract: Skin grafting is the routine standard of care to manage third degree burns and problematic skin defects. Several commercially available dermal substitutes and biologic skin equivalents are placed in the wound bed to facilitate the healing process of the skin grafts, as well as to provide mechanical support for the cells to grow and to delay the contracture. To study pathology and develop new therapies, an immune-competent rat model is required. We have created two different skin graft animal models to mimic the clinical skin grafting operation, the dorsum skin grafting (DG) and inguinal skin grafting (IG). To create a recipient site, a full-thickness, round excision wound was created on the dorsum between rats' scapular angles, covered with DG or IG. Graft contraction was quantified and tissue was harvested on predetermined time points for analysis. Histologic staining was performed to differentiate between DG and IG. Collagen deposition was assessed with Masson's trichrome staining. Mast cells were detected with Toluidine blue. Macrophages were stained with CD68 immune. Vascularity was assessed with functional vessels numbers. Cell proliferation was assessed with Ki67 immune. This model has all the advantages of murine models, such as an abundance of genetic variants and applicable tools, low cost, and practical housing techniques, all of which will promote the development of new therapies and testing new biologic skin equivalents and dermal substitutes.

Keywords: Skin graft, burns, animal model

Introduction

Wound repair and regeneration is a complicated process. Problematic wound healing often results in contraction and scarring, excessive contraction lead to contracture which may causes unfavorable complications such as disfigurement, pain, itching, psychological complications, and restriction of movement. These complications are devastating to both the patient and the physician and can negatively impact the quality of life. Compared to normal skin, these contractures are characterized by an aberrant color, local incrassation, irregular surface area, and a poor elasticity, which may require many corrective revision surgeries.

For patients where skin flap and full thickness skin graft (FTSG) anatomical harvest sites are

limited, split thickness skin graft (STSG) has been used as an alternative. Split thickness skin graft (STSG) is still considered the standard therapy for full-skin defects caused by trauma or surgical procedures [1, 2]. The survival of STSG includes several stages. Within three days after transplantation, the skin graft is mainly viable by oxygen and nutrients diffused from the underlying wound bed. After five days, angiogenesis and new blood vessels formed from the deep tissue make the skin graft remove debris and maintain the original structures. Various factors for improving STSG survival and delaying contracture have been introduced, such as autologous stem cells, growth factors, and synthetic agents. Although some success has been achieved, there are a lot of unsatisfying problems resulted from contractures. Therefore, the development of favor-

able methods to improve skin wound healing would still be the research focus in the field of biomedical materials [3]. This trend requires a reliable and effective animal model to evaluate their safety and efficacy, including biological compatibility, antigenicity, and their ability to repair dermal defect and accelerate re-epithelization and basement membrane formation [4, 6], as well as assessing novel therapies to improve the healing process.

In some studies, tests are performed in a porcine animal model with autologous split-thickness skin [7, 10]. It is well known that the study of the characteristics of an animal model is important to understand the advantages and limitations of this model, and to foster the development of superior models [11].

Conventionally, models to study contractures and dermal substitutes were performed in immune-deficient animals, in which several models have been used. In athymic rat model, the results showed that proliferating fibroblast was diminished when compared to human scars. Other models such as rabbits and mice, particularly genetic mutants, have been used to evaluate new therapeutic means. The rabbit ear excisional hypertrophic scar contracture (HSc) model was widely used for elucidating molecular pathways in HSc. Other animal models like chemically-induced hypertrophic scars in guinea pigs, show that the scar development was inconsistent and unpredictable between animals.

Large animals like pigs are expensive and challenging to house and handle, and thus are limited in the ability to test dermal substitutes. Animal models like rabbits and immune-deficient mice are also used in evaluating dermal substitutes, but own immunodeficiency make them vulnerable to infections and with high a degree of morbidity and mortality, limiting them as animal models, and the process of wound healing between immune deficient animals and human is significantly different.

Being the most widely used animals for biologic and biomaterial research, the rats are commercially available and are appropriate to provide a suitable platform of skin for wound studies. They have become a fundamental, low-cost research tool in numerous applications and their wound healing features have been widely acknowledged after years of effort.

In the current study, we have developed a novel rat skin graft model to simulate human skin grafting and evaluate dermal substitutes and biologic skin equivalents. This animal model is reproducible, convenient to maintain and can be useful to directly to test new therapies and drugs. The aim of this study was to set up a autologous skin graft model with a normal immune system. This model has the advantages of small animal models and can serve as a tool to study skin grafting, and scar contractures aiming to develop and test new therapies.

Materials and methods

Rats

Male Sprague-Dawley (SD) rats, weighing 180-200 gm, were obtained from the Laboratory Animal Center of Sun Yat-sen University. All rats in the study were monitored for signs of morbidity including significant unexpected loss of body weight, irritability, tachypnea and dyspnea. The animals were divided into three groups according to the different subsequent treatments of their wound bed: Tegaderm dressing (no skin graft), Dorsum graft (DG), and Inguinal graft (IG). The rats were randomized into one of the three groups (n = 20 per group). All rats were housed under the animal protocols approved by the Institutional Animal Care and Use Committee of the First Affiliated Hospital of Sun Yat-sen University.

Procedures

All rats were anesthetized using gas anesthesia (isoflurane, 2%, O_2, 2 L/min). Each rat was shaved with metallic clippers after induction of anesthesia.

Excisional wounds

Scrubbed by Betadine Veterinary Surgical Scrub with 70% alcohol, the dorsal skin of the rat was prepared for surgery. A diameter of 20 mm round full-thickness excisional wound was made on the dorsum of the rat using iris scissors under aseptic condition. For Tegaderm group, the wounds were covered by transparent Tegaderm film dressing (3M Health Care, St. Paul, MN, USA).

DG and IG transplantation

DG donor skin was created through excision the skin, and dissected away the deep partial der-

mis and the panniculus carnosus layer. The inguinal skin of the rat was sterilized by 70% alcohol, and a diameter of 20 mm round full-thickness excisional wound was made on the rat inguinal skin, which was the same as DG. The IG was obtained from the excised inguinal skin by getting rid of the deep partial dermis and the panniculus carnosus. By using a sharp tipped scalpel, evenly distributed fenestrations were created on the grafts for secretion drainage. The grafts were stitched to adjacent wound margin with interrupted sutures. Then a bolster dressing was placed on the top of the skin grafts to provide proper compression.

Postoperative care and gross examination

All rats were singly housed after surgery. For Tegaderm group, dressings were changed daily for the first 2 days and then removed on day 3. For DG and IG group, dressings were changed on day 3 postoperatively and removed by day 7. Those wounds/grafts were observed separately on days 0, 3, 7, 14, 21, and 28 postoperatively. The relative skin wounds/grafts size were calculated by gravitational planimetry using the following formula:

$$\text{Relative skin wound/graft size \%} = \frac{\text{Remaining skin wound/graft size}}{\text{Original skin wound/graft size}} \times 100\%$$

Tissue specimen collection

All animals were euthanized at the predetermined time points. The grafts/wounds and surrounding tissues were collected and divided into two parts along the center line. All specimens were immersed in 10% formalin and fixed at room temperature, and then dehydrated through a graded series of ethanol wash and clearing agent, finally embedded in paraffin. Prior to staining, tissue sections were dewaxed and rehydrated.

Histology

All sections were stained with hematoxylin and eosin (HE), Masson's Trichrome stain, and Toluidine blue stain following the manufacturer's (Sigma-Aldrich, Inc. t. Louis, MO, USA) standardized protocols.

Immunohistochemistry (IHC) CD68 and Ki67 staining

Immersed in 3% hydrogen peroxide (H_2O_2) for 10 min to inhibit endogenous peroxidase, tis-

sue sections were putted into citrate pH 6 antigen retrieval solution (Target Retrieval Solution, Dako North America Inc. Carpinteria, CA, USA) and placed into a 98°C water bath for 10 min, followed with 30 min cooling down at room temperature. After rinsing sections with deionized water and 1X tris-buffered saline (TBS, TBS Automation Washing Buffer, Biocare Medical, Concord, CA, USA), sections were blocked with Background Buster (Background Buster, Innovex BiosciencesRichmond, CA, USA) for 45 min at room temperature. This procedure is used to block non-specific antibody binding. Anti-CD68 (1:800 dilution, Bio-Rad Laboratories, Hercules, CA, USA) or anti-Ki67 antibody (1:200 dilution, Thermo Fisher Scientific, Waltham, MA, USA) was incubated for 1 h and then washed with TBS, the slides were stained following the manufacturer's standardized protocols of DAKO EnVision™ Detection System (Agilent Technologies, Santa Clara, CA, USA) for 30 min at room temperature. The nuclei were then blued by quickly dipping the slides in hematoxylin solution. The sections were then rinsed in tap water for 30 min.

Imaging and analysis

Hair follicles at low magnification were quantified by use of ImageJ software. Measurements of epidermal thickness [12], and microvessels and cell counting [13-15] in high-power field (HPF) were obtained by ImageJ software. The collagen deposition level was computed as collagen index which is equal to (=) (B + G)/(2R + B + G) for each pixel within the image (where R, B and G represent the red, blue, and green pixel values, respectively). The value of the collagen index ranged from 0 for extremely red objects to 1 for completely blue-green objects [16, 17]. Four stained sections in each group for each time point were visualized by an magscanner KF-PRO-005 (Konfoong Biotech International CO., LTD, NingBo, CN). In each section three random fields were selected for quantitative assay.

Statistical analysis

The results were statistically expressed as means ± standard deviations. Inter-group comparison was performed using the one-way ANOVA or the Student's t-test when appropriate. *$P<0.05$ was considered statistically significant.
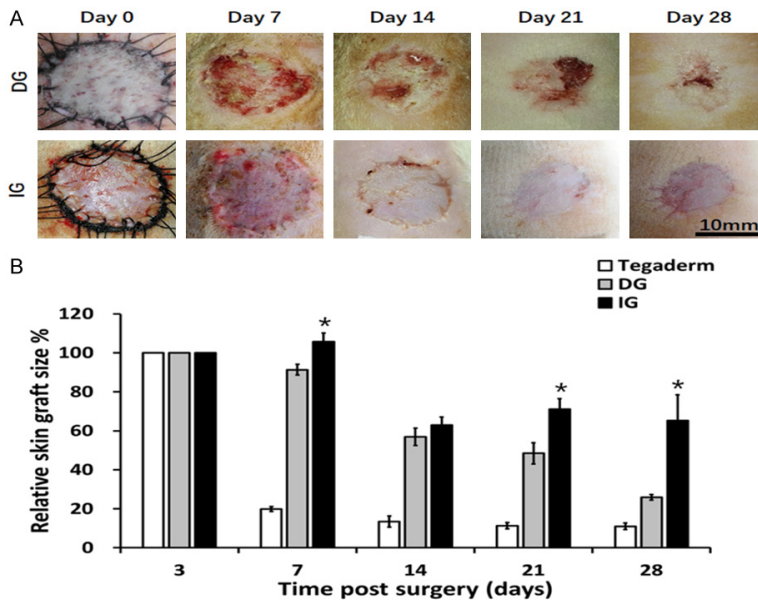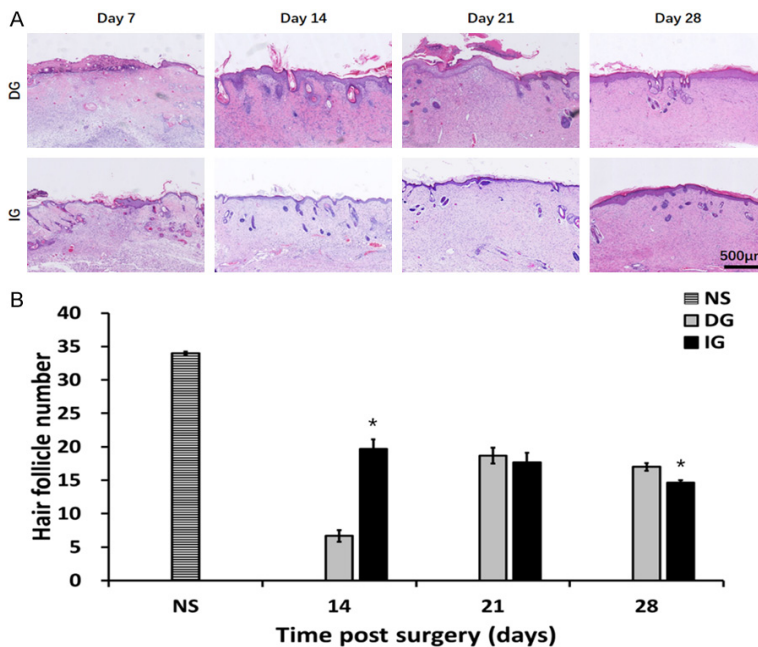
Figure 1. Contraction of different skin grafts: DG, IG. A. Morphology of skin grafts over 28 days post-surgery. B. Quantification of relative skin graft size. *P<0.05. Grafts of DG groups had contracted to 26% of their original size by day 28, whereas IG group remained 65% of the initial graft size.

Figure 2. The modification of skin appendages in different grafts. A. HE staining of epidermis section showing hair follicles, sebaceous glands. B. Quantification of hair follicles, *P<0.05.

Results

Skin graft survival

We have used immunocompetent rats in the study, because the immune system effect the healing process, and this also allows for wide usability of the model. Skin grafts were used from the same rat (autografts) to represent the same practice that is done in human skin grafting. Split-thickness skin graft are usually harvested using a dermatome in humans. We have tried to do the same in the rats in this study, but found the harvested layers to be inconsistent in quality and thickness. Using a gauze package as a pressure dressing is important for the skin graft survival, the bolster is used regularly in human skin grafting. The skin grafts were found to go through a variety of changes before they finally well taken (**Figures 1A**, **2A**).

Skin grafts survived without disappearing

Gross clinical observation of the grafts demonstrated that on 28, the DG contracted to 25.90±1.39%, while (P< 0.05) IG contracted to 65.18± 13.30% of the original wound size (**Figure 1B**). Wounds with no skin grafts have closed on 14 forming a visible scar (relative skin size: 12.87±1.56%). Qualitative gross assessment of the grafts revealed that the IG maintained better appearance with no visible ulceration in contrast with the DG which have demonstrated skin ulceration.
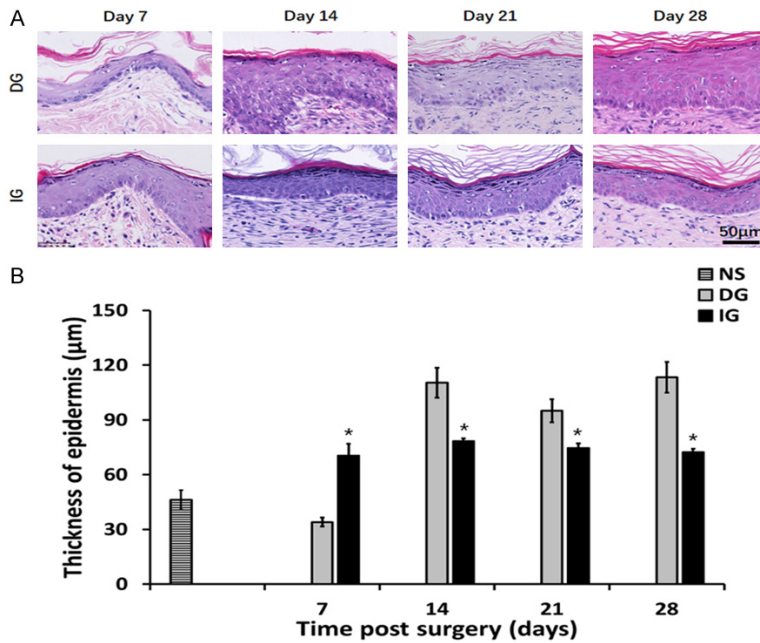
Alterations of skin appendages

The number of hair follicles in the skin grafts is demonstrated in **Figure 2B**. Small numbers of hair follicles (6.67± 0.88) were observed in the DG group at day 14. The hair follicles in the IG group were more preserved when compared to the DG grafts (P<0.05). Although hair follicles and sebaceous glands were still rare in all groups on day 28, DG grafts demonstrated higher numbers of
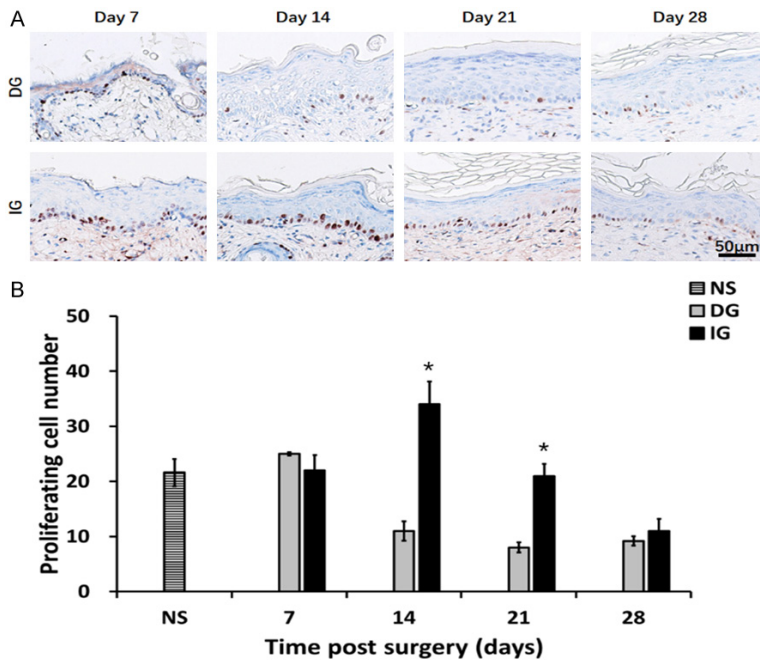
Figure 3. Characterization of epidermis thickness in different grafting groups. A. HE staining of epidermis. B. Thickness of epidermis on each observation point. *P<0.05.

Figure 4. Characterization of Ki67 positive cells in epidermis of different grafting groups. A. Ki67 staining of epidermis. Brown: Ki67 positive cell. B. Proliferation cell number of epidermis on different time point. *P<0.05. The IG group had the more proliferation cells by the day 14 and day 21.

Epidermal changes in the skin grafts

We have characterized the morphology of the epidermis in **Figure 3**. On the 7th day after the operation, the epidermis of the DG group was regenerative and thin (34.00± 2.42 μm). While the IG groups demonstrated a thicker epidermal layer (70.48±6.51 μm). On day 14, the reepithelialization was completed in all grafting groups. A noticeable increase was found in the epidermal thickness of all grafts (DG: 110.35±6.30 μm, IG: 78.30±2.45 μm). Starting day 14 to day 28 the epidermal thickness of the DG group was more than the IG groups (P<0.05), while the epidermis thickness of IG did not change significantly. The cellular proliferation in the epidermis was assessed with using Ki67 immune stain, which represents the nuclear antigen the is expressed in cells which are proliferating, the findings are demonstrated in **Figure 4A**. Compared to DG, IG demonstrated increase in the number of proliferating cells at all time, however the changes was statistically significant on days 14 and 21 (P<0.05) (**Figure 4B**).

*Collagen index showed increased degree of deposition in IG*

Compared to the DG, Masson's trichrome stain analysis of IG showed overall increases in collagen deposition (**Figure 5A**), by the day 14, day 21, day 28, we can see the statistical significance over the two groups (D14: IG 0.66±0.008, DG 0.59±0.007, P<0.05; D21: IG 0.67±0.01, DG 0.59±0.001, P<0.05; D28 IG 0.76±0.01,

skin appendages (17.00±0.58) than the number in the IG grafts (14.67±0.33) (P<0.05).
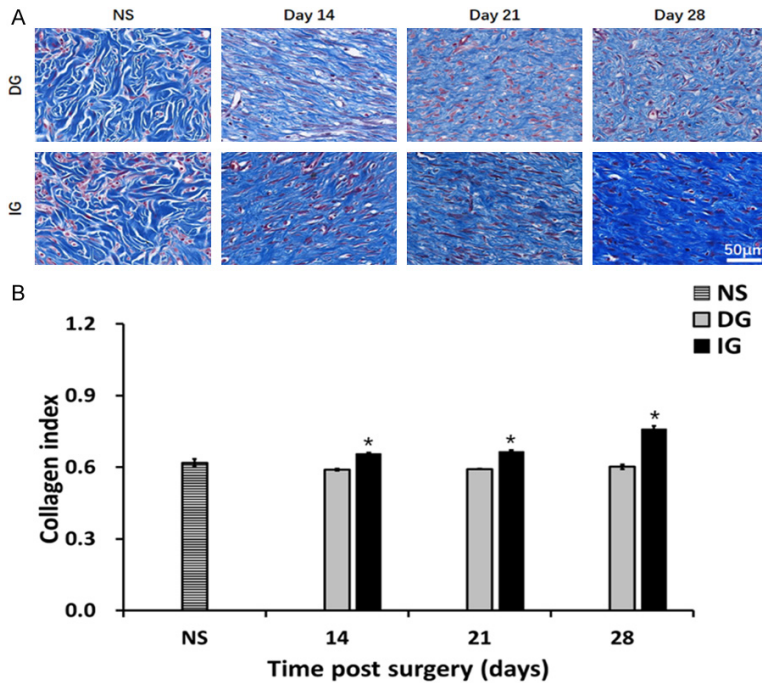
Figure 5. Collagen deposition in the skin graft and normal skin. A. Masson's trichrome staining on post operation day 14, day 21, day 28 and normal skin. B. Quantification of collagen intensity in the image. *$P<0.05$. The morphology and intensity of collagen fibers in IG are closer to that of skin scar tissue.
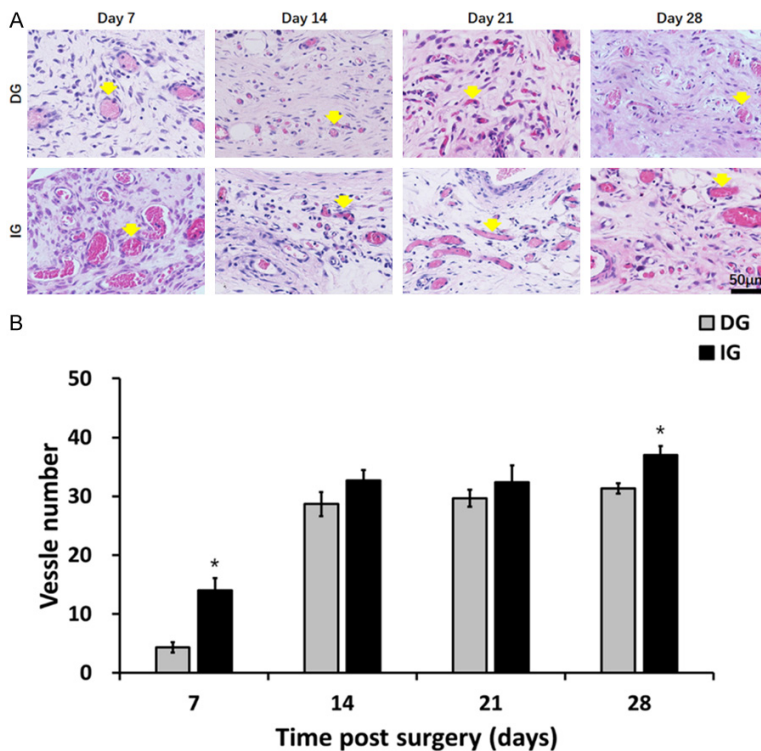
Figure 6. Characterization of angiogenesis of the skin grafts. A. HE staining displaying microvessels (indicated by yellow arrows) in the grafts at day 7, 14, 21 and 28. *$P<0.05$. B. In the day 7 and 28 post-surgery, the IG group showed higher microvessel number.

DG 0.60±0.01, $P<0.05$) (Figure 5B).

Skin grafts demonstrated increased vascular density

The rapidity of grafts vascularization is important in protection against infection. The microvascular density was clearly evident in all grafts (Figure 6A). Analysis showed increased number of blood vessels at all time points of the skin grafts, reflecting an increase in vascular density. The increases were statistically significant on day 7 and day 28 (day 7: DG 4.33±0.88, IG14.00± 2.08, $P<0.05$; day 28: DG 31.33±1.53, IG 37.00±1.53, $P<0.05$) (Figure 6B).

Skin grafts demonstrated increased macrophages and mast cells

Our analysis has demonstrated increased macrophage infiltration in all grafting groups (Figure 7A). Compared to the DG, an increased number of CD68 positive macrophages at all the time points was observed in the IG (day 7: DG 36.20±4.49, IG 75.00±12.21, $P<0.05$; day 14: DG 43.40± 5.71, IG 76.80±8.43, $P<0.05$; day 21: DG 25.60±1.21, IG 40.20±4.15, $P<0.05$; day 28 DG 17±2.70, IG 35.00±3.65, $P<0.05$) (Figure 7B). The analysis of the Toluidine blue stained-sections demonstrated increased numbers of mast cells in most time points in the skin grafts compared with the normal skin (Figure 8).

Discussion

Skin grafts are commonly used under unfavorable conditions causing skin loss, and in wounds with moderate infection or compromised blood supply which is not sufficient
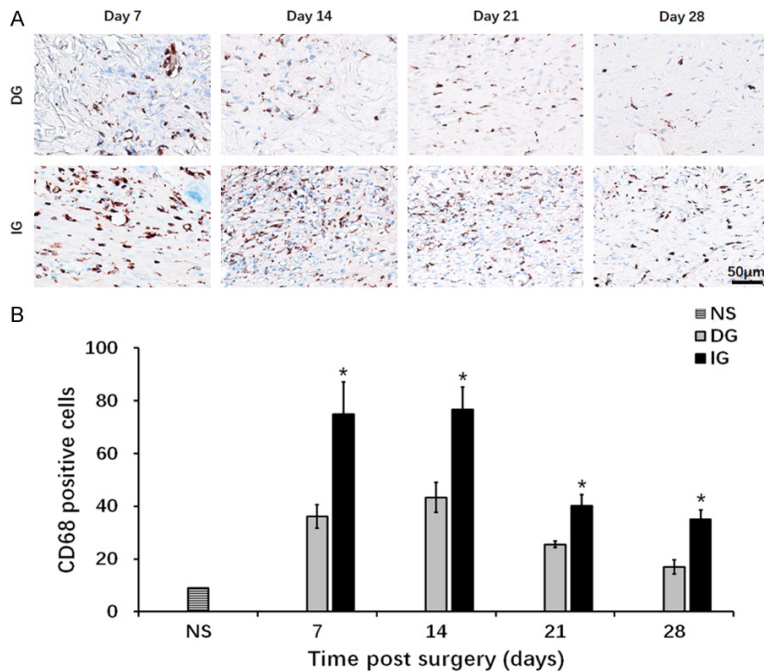
Figure 7. Presentation of CD68 positive cells of the granulation tissue underneath the skin graft. A. CD68 staining of macrophage cells. Blue: cell nucleus; brown: CD68 positive cell. B. Quantification of macrophage cells at day 7, day 14, day 21 and day 28. *P<0.05. The IG group showed more severe inflammation throughout the wound healing process.
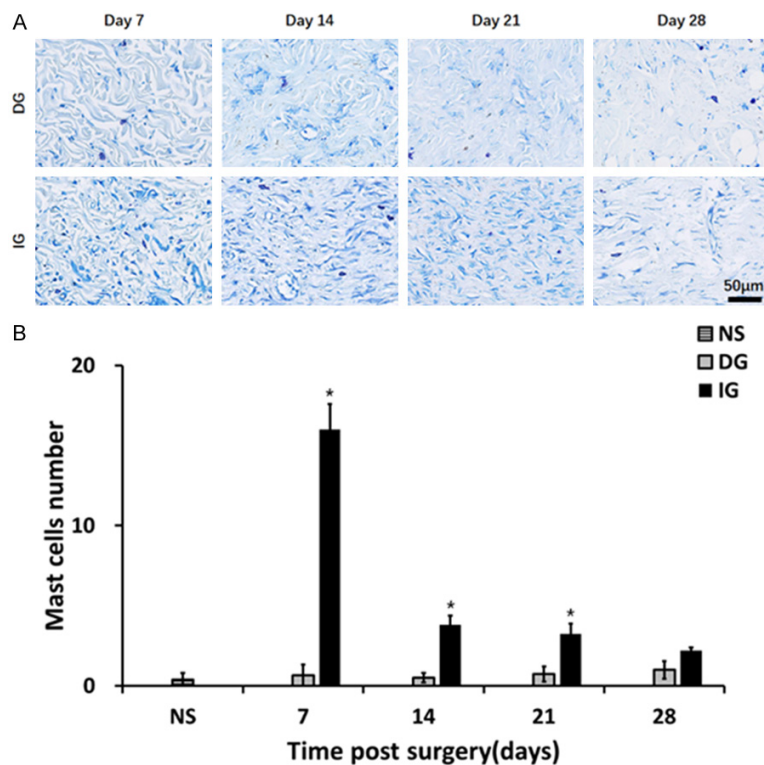
Figure 8. Infiltration of mast cells in the granulation tissue beneath the skin grafts. A. Toluidine blue staining of granulation tissue. Blue: nucleus; violet: mast cell. B. Quantification of mast cells at day 7, day 14, and day 21.

enough to support wound healing [18]. Extensive tissue damage and skin loss caused by third degree burns is usually treated by escharectomy and skin grafting. These wounds often heal by forming scars and contractures, when used alone. Dermal substitutes are sometimes placed in the wound bed to facilitate the wound healing process, as well as to provide mechanical support for the cells to grow and to increase the skin grafts survival. Continuous efforts are ongoing to develop new dermal substitutes and biologic skin equivalents; therefore, there is a need to have a validated, easy and cost-effective animal model to study new therapies. Porcine model is the preferred model in skin wound healing studies [19, 20]. The structure of the epidermal and dermal layer of porcine skin closely matches that of the human skin [21] and wounds with size similar to human beings can be acquired by using this model. However, swine models require extensive animal research technical experience, impose high cost of housing and maintenance of the pig, and also pigs lack lots of the analytic tools available for smaller animals, which impacts their widespread application. On the other hand, the rodent remains widely used animal for scientific research because of its ease of operation, cost advantage, and abundance of mouse-specific reagents and genetic tools. Also, it is more effective and simple to use smaller animals as research

models before moving forward to bigger animals such as porcine. Our aim was to develop and validate a rat model of STSG that could be used to provide research direction for wound healing mechanism, and to test novel therapies and biologic skin equivalents to improve the outcomes of these procedures.

Immune system plays a critical role in wound repair [22, 23], so we chose immune competent rat to develop an STSG model in this study to simulate human wound healing processes with the associated inflammatory and immune response [24].

We have tried using harvesting the skin graft donor tissue from multiple anatomical sites of the rat, and we found that the most suitable skin grafts are those harvested from the dorsal and inguinal skin. To prepare the harvested skin to use as a skin graft, deep partial dermis and the panniculus carnosus were removed by using iris scissors to attain STSG grafts (DGs and IGs). These two grafts were uniform and their thickness can be compared with human skin split-thickness grafts. A sharp tipped scalpel was then used to create evenly spaced fenestrations on the grafts. To prepare the recipient site, full-thickness, round excisional wounds (20 mm in the diameter) were prepared in the dorsum of the rats, then skin grafts were transplanted and dressed with bolster like what is used in human skin graft procedures.

Skin graft contraction measurement started on post-operative day 7, after removing the bolster and followed up till day 28 post-operatively, this is because it has been reported before that the grafted wounds tend to stabilize within 4 weeks after the operation [25].

At the end of the study, we harvested skin grafts specimens and our histological analysis has demonstrated more reaction in the IG compared to the DG, as characterized by increased inflammatory response, neovascularization, proliferation and collagen deposition.

Harvested STSG does not carry its own blood supply. It passively absorbs the nutrients diffused from the wound bed initially [26, 27], then, its survival relies on new blood vessels from the recipient wound bed. The lower microvessel number in the DG group at an early stage (postoperative day 7) implied a slow

progress of vascularization. This phenomenon could be the result of integrative action of inflammation provoked by necrotic cells (**Figure 2**) and constituents of the dermis preserved in DG grafts (skin stem cells and extracellular matrix) [28-30]. As opposed to its early stage, a higher density of microvessels has been observed in the IG grafts (**Figure 6**), in the meanwhile, we also observed a higher inflammatory cell density as demonstrated by the increased infiltration of macrophages and mast cells (**Figures 7**, **8**). Although it is understood that increase in vascularity will contribute to a good IG take, prior studies have indicated that increased vascularity could account for the ongoing high inflammatory cell density and may eventually lead to skin fibrosis or hypertrophic scaring [31, 32].

Seven days after operation, the number of skin appendages, especially sebaceous glands, significantly decreased in DG and IG grafts (**Figure 2**). Such a pathologic condition was probably caused by the implantation operation and inadequate blood flow to the grafts. The graft structure and appendages of the IG group were better noticed in the early days post grafting. By day 14, new skin appendages started to appear again in both types of grafts, but they then gradually disappeared along with the deposition of collagen fibers.

Inflammatory cells, microvessels and fibroblasts are three major constituents of a critically important transitional connective tissue called granulation tissue [33]. Fibroblasts are actibated and differentiate in to contractile and secretory myofibroblasts (secrete extracellular matrix, ECM). Overgrowth of vascularized and collagenous granulation tissue is known to be associated with graft fibrosis [34, 35]. Along with the persistence of abundant inflammatory cells and granulation tissue in IG group, we observed excessive deposited, densely packed collagen fibers (**Figure 5**). The inflammatory stimulus also tends to unduly influence the proliferation resulting in a pro-fibrotic response. The initial high epiderm proliferation (**Figure 4**) and hyperplastic dermis in the IG group persisted through the end of study. Our results are similar to previous reports [36].

Ibrahim *et al*, has introduced a similar skin grafting murine model immune-competent mice. They created a third-degree burn on the

dorsum of mice and excised the injured tissue three days later. However, they have used ears from another donor mouse to graft, which makes the murine model non-autologous skin graft model with much smaller wound sizes [37]. The current rat model was developed to mimic larger-size wounds requiring autologous skin grafts and/or dermal substitutes. As a reasonable model for human skin grafting, many characteristics of our rat skin grafting model are similar to that of human in clinical practice. Human skin grafts are usually harvested through using a dermatome, which is not the case for our model, because our attempts to harvest skin grafts using a dermatome in rats was technically challenging and unreliable. The rate of rat skin graft (both DG and IG) contraction was significantly faster than what is reported in human [38]. Additionally, the scarred grafts in our model was flat with close to normal appearance.

We have introduced a novel, validated, immune competent, rat skin graft model which has been closely modeled after standard of human skin grafts and procedure. This autologous skin graft model has all the advantages of mice models and can be used in the research and development of new therapies and testing new biologic skin equivalents and dermal substitutes.

Disclosure of conflict of interest

None.

Abbreviations

DG, dorsum skin grafting; IG, inguinal skin grafting; BM, basement membrane; STSG, Split thickness skin graft; SD, Sprague-Dawley; HE, hematoxylin and eosin; H_2O_2, hydrogen peroxide; TBS, tris-buffered saline; IHC, immunohistochemistry; HPF, high-power field; HSc, hypertrophic scar contracture; ECM, extracellular matrix.

Address correspondence to: Drs. Shaohai Qi and Lei Chen, Department of Burns, The First Affiliated Hospital of Sun Yat-sen University, Guangzhou 510080, China. E-mail: qishaohaigzburns@163.com (SHQ); chenlei8@mail.sysu.edu.cn (LC)

References

[1] Schiestl C, Stiefel D, Meuli M. Giant naevus, giant excision, eleg(i)ant closure? reconstructive surgery with integra artificial skin® to treat giant congenital melanocytic naevi in children. J Plast Reconstr Aesthetic Surg 2010; 63: 610-615.5.

[2] Schiestl C, Neuhaus K, Biedermann T, Böttcher-Haberzeth S, Reichmann E, Meuli M. Novel treatment for massive lower extremity avulsion injuries in children: slow, but effective with good cosmesis. Eur J Pediatr Surg 2011; 21: 106-10.

[3] Zhong SP, Zhang YZ, Lim CT. Tissue scaffolds for skin wound healing and dermal reconstruction. Wiley Interdiscip Rev Nanomed Nanobiotechnol 2010; 2: 510-25.

[4] Yang L, Shirakata Y, Shudou M, Dai X, Tokumaru S, Hirakawa S, Sayama K, Hamuro J, Hashimoto K. New skin-equivalent model from de-epithelialized amnion membrane. Cell Tissue Res 2006; 326: 69-77.

[5] Dorsett-Martin WA. Rat models of skin wound healing: a review. Wound Repair Regen 2004; 12: 591-9.

[6] Yi JY, Yoon YH, Park HS, Kim CH, Kim CH, Kang HJ, Lee EA, Kim YY, Jin YJ, Kim TH, Son YS. Reconstruction of basement membrane in skin equivalent; role of laminin-1. Arch Dermatol Res 2001; 293: 356-62.

[7] Lamme EN, Van Leeuwen RTJ, Mekkes JR, Middelkoop E. Allogeneic fibroblasts in dermal substitutes induce inflammation and scar formation. Wound Repair Regen 2002; 10: 152-60.

[8] Philandrianos C, Andrac-Meyer L, Mordon S, Feuerstein JM, Sabatier F, Veran J, Magalon G, Casanova D. Comparison of five dermal substitutes in full-thickness skin wound healing in a porcine model. Burns 2012; 38: 820-9.

[9] Middelkoop E, Van Den Bogaerdt AJ, Lamme EN, Hoekstra MJ, Brandsma K, Ulrich MM. Porcine wound models for skin substitution and burn treatment. Biomaterials 2004; 25: 1559-67.

[10] Van Den Bogaerdt AJ, Ulrich MM, Van Galen MJ, Reijnen L, Verkerk M, Pieper J, Lamme EN, Middelkoop E. Upside-down transfer of porcine keratinocytes from a porous, synthetic dressing to experimental full-thickness wounds. Wound Repair Regen 2004; 12: 225-34.

[11] Ferreira LM, Hochman B, Barbosa MV. [Experimental models in research]. Acta Cir Bras 2005; 20 Suppl 2: 28-34.

[12] Svensjo T, Pomahac B, Yao F, Slama J, Eriksson E, Hunt TK. Accelerated healing of full-thickness skin wounds in a wet environment. Plast Reconstr Surg 2000; 106: 602-12.

[13] Kyriakides TR, Wulsin D, Skokos EA, Fleckman P, Pirrone A, Shipley JM, Senior RM, Bornstein P. Mice that lack matrix metalloproteinase-9 display delayed wound healing associated with delayed reepithelization and disordered collagen fibrillogenesis. Matrix Biol 2009; 28: 65-73.

[14] Javazon EH, Keswani SG, Badillo AT, Crombleholme TM, Zoltick PW, Radu AP, Kozin ED, Beggs K, Malik AA, Flake AW. Enhanced epithelial gap closure and increased angiogenesis in wounds of diabetic mice treated with adult murine bone marrow stromal progenitor cells. Wound Repair Regen 2007; 15: 350-9.

[15] Di-Poï N, Ng CY, Tan NS, Yang Z, Hemmings BA, Desvergne B, Michalik L, Wahli W. Epithelium-mesenchyme interactions control the activity of peroxisome proliferator-activated receptor beta/delta during hair follicle development. Mol Cell Biol 2005; 25: 1696-712.

[16] Ibrahim MM, Chen L, Bond JE, Medina MA, Ren L, Kokosis G, Selim AM, Levinson H. Myofibroblasts contribute to but are not necessary for wound contraction. Lab Invest 2015; 95:1 429-38.

[17] Olbrich KC, Meade R, Bruno W, Heller L, Klitzman B, Levin LS, Friedman HI, Bruno W, Mast BA. Halofuginone inhibits collagen deposition in fibrous capsules around implants. Ann Plast Surg 2005; 54: 293-6.

[18] Nie C, Yang D, Xu J, Si Z, Jin X, Zhang J. Locally administered Adipose-derived stem cells accelerate wound healing through differentiation and vasculogenesis. Cell Transplant 2011; 20: 205-16.

[19] Sullivan TP, Eaglstein WH, Davis SC, Mertz P. The pig as a model for human wound healing. Wound Repair Regen 2001; 9: 66-76.

[20] Branski LK, Mittermayr R, Herndon DN, Norbury WB, Masters OE, Hofmann M, Traber DL, Redl H, Jeschke MG. A porcine model of full-thickness burn, excision and skin autografting. Burns 2008; 34: 1119-27.

[21] Abdullahi A, Amini-Nik S, Jeschke MG. Animal models in burn research. Cell Mol Life Sci 2014; 71: 3241-55.

[22] Portou MJ, Baker D, Abraham D, Tsui J. The innate immune system, toll-like receptors and dermal wound healing: a review. Vascul Pharmacol 2015; 71: 31-6.

[23] Sun BK, Siprashvili Z, Khavari PA. Advances in skin grafting and treatment of cutaneous wounds. Science 2014; 346: 941-5.

[24] Rose LF, Wu JC, Carlsson AH, Tucker DI, Leung KP, Chan RK. Recipient wound bed characteristics affect scarring and skin graft contraction. Wound Repair Regen 2015; 23: 287-96.

[25] Boyce ST, Glafkides MC, Foreman TJ, Hansbrough JF. Reduced wound contraction after grafting of full-thickness burns with a collagen and chondroitin-6-sulfate (GAG) dermal skin substitute and coverage with biobrane. J Burn Care Rehabil 1988; 9: 364-70.

[26] Azzopardi EA, Boyce DE, Dickson WA, Azzopardi E, Laing JH, Whitaker IS, Shokrollahi K. Application of topical negative pressure (vacuum-assisted closure) to split-thickness skin grafts: a structured evidence-based review. Ann Plast Surg 2013; 70: 23-9.

[27] Horch RE, Bannasch H, Stark GB. Transplantation of cultured autologous keratinocytes in fibrin sealant biomatrix to resurface chronic wounds. Transplant Proc 2001; 33: 642-4.

[28] Ema H, Suda T. Two anatomically distinct niches regulate stem cell activity. Blood 2012; 120: 2174-81.

[29] Fuchs E. Scratching the surface of skin development. Nature 2007; 445: 834-42.

[30] Watt FM, Jensen KB. Epidermal stem cell diversity and quiescence. EMBO Mol Med 2009; 1: 260-7.

[31] Wang J, Ding J, Jiao H, Honardoust D, Momtazi M, Shankowsky HA, Tredget EE. Human hypertrophic scar-like nude mouse model: characterization of the molecular and cellular biology of the scar process. Wound Repair Regen 2011; 19: 274-85.

[32] Lupher ML Jr, Gallatin WM. Regulation of fibrosis by the immune system. Adv Immunol 2006; 89: 245-88.

[33] Desmoulière A, Redard M, Darby I, Gabbiani G. Apoptosis mediates the decrease in cellularity during the transition between granulation tissue and scar. Am J Pathol 1995; 146: 56-66.

[34] Gurtner G, Werner S, Barrandon Y, Longaker M. Wound repair and regeneration. Nature 2008; 453: 314-21.

[35] Martin P, Nunan R. Cellular and molecular mechanisms of repair in acute and chronic wound healing. Br J Dermatol 2015; 173: 370-8.

[36] Hinshaw JR, Miller ER. Histology of healing split-thickness, full-thickness autogenous skin grafts and donor sites. Arch Surg 1965; 91: 658-70.

[37] Ibrahim MM, Bond J, Bergeron A, Miller KJ, Ehanire T, Quiles C, Lorden ER, Medina MA, Fisher M, Klitzman B, Selim MA, Leong KW, Levinson H. A novel immune competent murine hypertrophic scar contracture model: a tool to elucidate disease mechanism and develop new therapies. Wound Repair Regen 2014; 22: 755-64.

[38] Quilichini J, Benjoar MD, Hivelin M, Lantieri L. Split-thickness skin graft harvested from the scalp for the coverage of extensive temple or forehead defects in elderly patients. Arch Facial Plast Surg 2012; 14: 137-9.